Adaptive Generalized Sidelobe Canceler Beamforming With Time-Varying Direction-of-Arrival Estimation for Arrayed Sensors

Dah-Chung Chang, *Senior Member, IEEE*, and Bo-Wei Zheng

***Abstract*—Adaptive generalized sidelobe cancelers (GSCs) have been widely used to enhance the desired signal and instantaneously suppress interference signal and noise. However, the GSC beamforming method must know the direction of arrival (DOA) of the desired signal in advance. In this paper, we consider the case of a sensor array application in free-field air in which the target signal source is moving, leading to a time-varying DOA problem. Through analysis of the GSC output error signal, we propose an effective method for estimating the time-varying DOA for a GSC. The new method avoids the intensive complexity requirements of conventional DOA estimation algorithms such as the multiple signal classification algorithm and estimation of signal parameters via rotational invariant techniques. In addition, the convergence performance of adaptive GSC algorithms suffers from an error signal in the presence of the desired signal. A simple augmented Kalman filter (AKF) is employed to calculate the beamformer's weighting coefficients, removing the influence of the desired signal from the GSC output to improve the convergence performance. A simulation evaluation of the signal-to-interference-plus-noise ratio (SINR) revealed that the AKF algorithm combined with the new DOA tracking method has a better convergence rate and SINR performance than other adaptive GSC algorithms of similar complexity such as the standard Kalman filter and recursive least squares.**

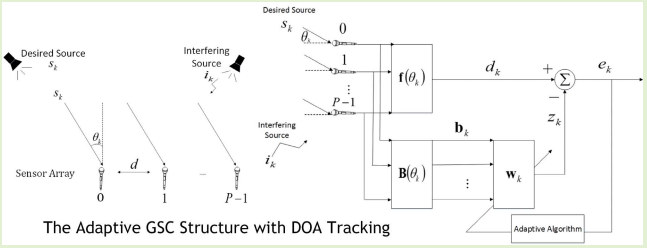

The Adaptive GSC Structure with DOA Tracking

***Index Terms*— Beamforming, generalized sidelobe canceler (GSC), sensor array, direction-of-arrival (DOA), Kalman filter (KF).**

I. Introduction

ADVANCED signal processing technologies with sensor arrays have attracted considerable interest for the suppression of interfering signals in communication, radar, and microphone applications [1]–[4]. In a real-world environment, a received signal is usually composed of the desired signal sent from the target source and unwanted signals emitted by another source that causes interference. The interfering signals can significantly degrade the performance of obtaining the desired signal. The collaborative beamforming method uses multiple sensors for efficient power usage to improve this performance [5]–[7]. With multiple sensors, interference reduction is usually realized through adaptive beamforming such as with a generalized sidelobe canceler (GSC) [3], [8], [9]. The main concept of this beamforming technique is to maximize the gain of the array output in the direction of the desired signal while minimizing gains in the directions of interfering signals by adjusting the weighting vector of the beamformer.

From a theoretical perspective, the minimum variance distortionless response (MVDR) criterion based on the linearly constrained minimum variance method [10] provides the optimum solution to beamforming problems, provided that the direction of arrival (DOA) of the desired signal is known *a priori*. However, the MVDR beamformer must calculate the inverse of the autocovariance matrix of the array input signal, but the accurate value is not easy to obtain. Instead, the GSC method combined with adaptive filters is more efficient and has lower computational cost. Some recursive algorithms such as the least mean square (LMS) [11], recursive least square (RLS) [12], [13], and Kalman filter (KF) [14], [15] algorithms are usually applied to implement a GSC. Notably, the aforementioned adaptive algorithms are developed to recursively

Manuscript received November 16, 2019; accepted December 17, 2019. Date of publication December 25, 2019; date of current version March 17, 2020. This work was supported in part by Qualcomm Technologies, Inc., under Grant NAT-414678. The associate editor coordinating the review of this article and approving it for publication was Dr. Rosario Morello. *(Corresponding author: Dah-Chung Chang.)*

Dah-Chung Chang is with the Department of Communication Engineering, National Central University, Taoyuan 32001, Taiwan (e-mail: dcchang@ce.ncu.edu.tw).

Bo-Wei Zheng is with XYZprinting Inc., New Taipei 22201, Taiwan (e-mail: spy311551@gmail.com).

Digital Object Identifier 10.1109/JSEN.2019.2962215

adjust their filter coefficients by minimizing the error signal; that is, the convergent direction of the algorithm is led by a small error signal. Conventionally, the adaptive GSC method uses the GSC output as the error signal to converge the weighting vector of the beamformer, which may result in robustness and convergence problems if the GSC output contains the desired signal.

Furthermore, the performance of the conventional GSC is only guaranteed when the exact DOA of the desired signal is known because a mismatched DOA results in performance loss. A variety of DOA estimation problems have been studied in the field of signal processing for sensor arrays [16]–[18]. DOA estimates can be obtained using some typical offline algorithms, such as the multiple signal classification (MUSIC) algorithm [19], [20] and the estimation of signal parameters via rotational invariance technique (ESPRIT) [21], [22]. However, these methods often incur a heavy computational load if the DOA of the target source is time-varying and requires tracking. For the purpose of simplicity, some suboptimal methods haven been proposed. For example, an approximate maximum likelihood approach was proposed for acoustic DOA estimation [23]. As shown in [24], the DOA can be obtained by taking advantage of the symmetrical planar array about two axes in a three-dimensional monopulse radar system, and a reduced-dimension GSC structure can reportedly offer effective suppression of interference. Some robust and adaptive methods have been proposed to cope with the DOA mismatch problem [25]–[28]. Those methods are mainly based on using an MVDR beamformer to determine the beamforming coefficients while applying optimization schemes. In speech and acoustic applications, a disadvantage of the optimization process is excessive cost due to the high computational power required for digital signal processing (DSP). Hence, an efficient DOA tracking algorithm applicable to the adaptive GSC structure, such as a KF-based GSC for interference cancellation, would be favorable for addressing the time-varying DOA engendered by a moving source.

In this paper, a new DOA tracking method based on the GSC output error signal is proposed for adaptive GSC beamforming. A new KF-based GSC algorithm combined with the DOA tracking method is simulated under the scenario of a moving target signal source along with multiple interfering signals for enhancing the signal-to-interference-plus-noise ratio (SINR). There are two main features of this work that are worth noting:

- We assume that an approximate estimate of the DOA of the target signal source is given in advance, and the DOA is time-varying because the target source moves. In our framework, the KF-based GSC model is developed on the basis of the DOA parameter. Taking into consideration the DOA mismatch, we can observe from the SINR analysis of the GSC that even when the beamformer's weighting vector is accurately known, thus eliminating interfering signals, the DOA mismatch still increases the noise power such that the GSC output signal-to-noise ratio (SNR) decreases. Therefore, we propose a new DOA tracking algorithm that can be applied along with the GSC operation without any training signal, thus avoiding the intensive computational complexity required in the conventional MUSIC algorithm and ESPRIT for DOA estimation.
- An augmented KF (AKF) approach [29] is applied to estimate both the beamformer's weighting vector and the signal of the moving target. Using the estimated target signal, the AKF algorithm can reduce the influence of the desired signal at the GSC output such that the SINR performance of the new AKF GSC is improved. The complexity of a conventional KF is known to be subject to the computation of the inverse matrix, the size of which depends on the dimension of the observation equation in the KF. However, because of its remarkable simplicity, the AKF developed in this paper only requires a 2×2 matrix inversion. Therefore, it is suited to practical implementation with DSP.

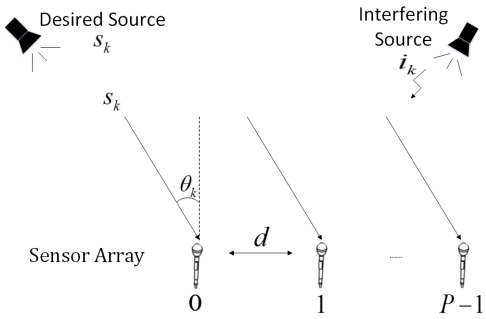

Fig. 1. System concept of the sensor array.

The simulation results reveal that, except for the lack of performance improvement resulting from the target signal source approaching the interfering signals, the proposed DOA tracking algorithm provides satisfying estimation performance; moreover, the AKF has a faster convergence rate and better SINR performance than the conventional KF and RLS algorithms at the same computational complexity. Furthermore, the proposed DOA estimation method has sufficient estimation robustness and does not lose track of the target signal as the source moves in the directions of interfering signals.

The remainder of this paper is organized as follows. Section II describes our system model, where the GSC structure is delineated by introducing the Wiener solution to the beamformer's weighting vector. In Section III, the errors caused by DOA mismatch are separated from the ideal results of the beamforming vector and the blocking matrix when giving a precise DOA. We can observe how those mismatch errors produce the effect of DOA mismatch on the GSC output signal, with which the time-varying DOA can be estimated using a recursive equation proposed in this paper. The AKF method to obtain the beamforming vector is introduced in Section IV. Simulation results are explained in Section V. Section VI provides the conclusions of this work.

II. System Model

As depicted in Fig. 1, P uniformly distributed sensors are employed to enhance the desired signal s_k by suppressing the interfering signal i_k when the DOA θ_k of the impinging target source is different from those of the interfering signals, where k is the sample index. Define the pth element $a_p(\theta_k)$ in the

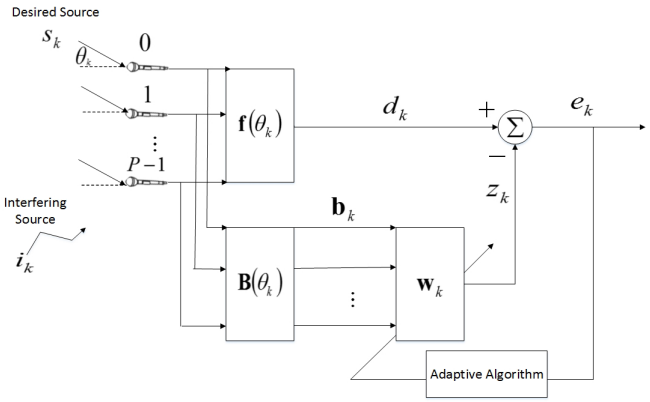

Fig. 2. GSC structure of the sensor array with a time-varying DOA.

steering vector for the P arrayed sensors as

$$a_p(\theta_k) = e^{-jp\frac{2\pi}{\lambda}d\sin\theta_k} \tag{1}$$

where $p = 0, 1, \cdots, P-1$, λ is the wavelength of the desired signal, d is the distance between any two adjacent sensors and $d \le \frac{\lambda}{2}$ to prevent spatial aliasing. The received signal of the pth sensor can be written as

$$r_{p,k} = a_p(\theta_k)s_k + i_{p,k} + n_{p,k} \tag{2}$$

where $i_{p,k}$ is the interfering signal for the pth sensor and $n_{p,k}$ is the additive white Gaussian noise (AWGN) with variance σ_n^2.

To express the received signal collected from the P sensors in vector form, we have

$$\mathbf{r}_k = \mathbf{a}(\theta_k)s_k + \mathbf{i}_k + \mathbf{n}_k, \tag{3}$$

where the received signal vector $\mathbf{r}_k = [r_{0,k}, r_{1,k}, \cdots, r_{P-1,k}]^T$, steering vector $\mathbf{a}(\theta_k) = [a_0(\theta_k), a_1(\theta_k), \cdots, a_{P-1}(\theta_k)]^T$, interfering signal vector $\mathbf{i}_k = [i_{0,k}, i_{1,k}, \cdots, i_{P-1,k}]^T$, and noise vector $\mathbf{n}_k = [n_{0,k}, n_{1,k}, \cdots, n_{P-1,k}]^T$.

Our problem formulation follows that the location of s_k is moving along with interfering signals $\mathbf{i}_k$; thus, the time-varying DOA θ_k must be tracked. Consider the GSC structure depicted in Fig. 2; the $P \times 1$ beamforming vector $\mathbf{f}(\theta_k) = [f_0(\theta_k), f_1(\theta_k), \cdots, f_{P-1}(\theta_k)]^T$ is used to calculate the optimal combination of received signals to obtain the desired signal through the steering vector $\mathbf{a}(\theta_k)$. According to [30], we have

$$\mathbf{f}(\theta_k) = \frac{1}{P}\mathbf{a}(\theta_k). \tag{4}$$

The output d_k is then written as $d_k = \mathbf{f}^H(\theta_k) \cdot \mathbf{r}_k$. However, d_k contains the interfering signals. The $P \times (P-1)$ matrix $\mathbf{B}(\theta_k)$ in the lower branch of the GSC is referred to as the blocking matrix, whose purpose is to eliminate the desired signal from the array input by nulling the space of $\mathbf{a}(\theta_k)$. According to [31], the design of $\mathbf{B}(\theta_k)$ can be

$$\mathbf{B}(\theta_k) = \begin{bmatrix} -\frac{a_1^*(\theta_k)}{a_0^*(\theta_k)} & -\frac{a_2^*(\theta_k)}{a_0^*(\theta_k)} & \cdots & -\frac{a_{P-1}^*(\theta_k)}{a_0^*(\theta_k)} \\ 1 & 0 & \cdots & 0 \\ 0 & 1 & \cdots & 0 \\ \vdots & \vdots & \ddots & \vdots \\ 0 & 0 & \cdots & 1 \end{bmatrix}. \tag{5}$$

The output of the blocking matrix is a $(P-1)\times 1$ vector, which can be expressed as $\mathbf{b}_k = \mathbf{B}^H(\theta_k) \cdot \mathbf{r}_k$. The coefficients of the $(P-1)\times 1$ weighting vector $\mathbf{w}_k = [w_{0,k}, w_{1,k}, \cdots, w_{P-2,k}]^T$ are adaptively adjusted to provide the output $z_k = \mathbf{w}_k^H\mathbf{b}_k$, with which the interfering signals contained in d_k can be perfectly removed through subtraction, such that the remaining error signal e_k is only the desired signal and noise. That is,

$$\begin{aligned} e_k &= d_k - z_k \\ &= \mathbf{f}^H(\theta_k)\mathbf{r}_k - \mathbf{w}_k^H\mathbf{B}^H(\theta_k)\mathbf{r}_k \\ &= \mathbf{w}_{\text{gsc}}^H(\theta_k)\mathbf{r}_k, \end{aligned} \tag{6}$$

where the $P \times 1$ vector $\mathbf{w}_{\text{gsc}}(\theta_k) = \mathbf{f}(\theta_k) - \mathbf{B}(\theta_k)\mathbf{w}_k$ can be viewed as the overall beamformer's weighting vector.

In general, the GSC tends to determine the optimal weighting vector $\mathbf{w}_k$ by minimizing the cost function $J = \mathbb{E}[|e_k|^2]$, where $\mathbb{E}[\cdot]$ denotes the expectation, which is an unconstrained optimization problem,

$$\min_{\mathbf{w}_k} J = \min_{\mathbf{w}_k} \mathbf{w}_{\text{gsc}}^H(\theta_k)\mathbf{R}_{\mathbf{rr}}\mathbf{w}_{\text{gsc}}(\theta_k), \tag{7}$$

where $\mathbf{R}_{\mathbf{rr}} = \mathbb{E}[\mathbf{r}_k\mathbf{r}_k^H]$. By setting the first derivative of J to zero with respect to $\mathbf{w}_k$, we obtain the optimal solution

$$\mathbf{w}_{\mathbf{opt},k} = \left[\mathbf{B}^H(\theta_k)\mathbf{R}_{\mathbf{rr}}\mathbf{B}(\theta_k)\right]^{-1}\mathbf{B}^H(\theta_k)\mathbf{R}_{\mathbf{rr}}\mathbf{f}(\theta_k). \tag{8}$$

The result (8) is referred to as the Wiener solution, which is optimal for Gaussian noise. Because of the intensive matrix inversion operation and the prerequisite of knowing the statistics $\mathbf{R}_{\mathbf{rr}}$, (8) is not feasible in practical application.

III. New DOA Estimation Method for a GSC

A. Effect of Mismatched DOA

In the ideal case, the DOA of the desired signal should be known for a GSC in advance and is usually considered either a stationary source or a given accurate DOA initialization. Revisiting (6), by substituting (3) into (6), we have

$$\begin{aligned} e_k &= \mathbf{w}_{\text{gsc}}^H(\theta_k)\mathbf{a}(\theta_k)s_k + \mathbf{w}_{\text{gsc}}^H(\theta_k)\mathbf{i}_k + \mathbf{w}_{\text{gsc}}^H(\theta_k)\mathbf{n}_k \\ &= s_k + \mathbf{w}_{\text{gsc}}^H(\theta_k)\mathbf{n}_k \end{aligned} \tag{9}$$

where $\mathbf{w}_{\text{gsc}}^H(\theta_k)\mathbf{a}(\theta_k) = 1$ because $\mathbf{B}(\theta_k)$ nulls $\mathbf{a}(\theta_k)$, and $\mathbf{w}_{\text{gsc}}^H(\theta_k)\mathbf{i}_k = 0$ when $\mathbf{w}_k$ is ideal. That is, if the DOA is perfectly known for the GSC, then the ideal GSC output approaches s_k with a small and independent cancellation error noise. Let $P_{\text{s}} = \mathbb{E}[|s_k|^2]$ and $\sigma_n^2 = \mathbb{E}[\mathbf{n}_k^H\mathbf{n}_k]$; the total GSC output power can then be written as $P_{\text{e}} = P_{\text{s}} + P_{\text{n}}$, where $P_{\text{n}} = \mathbf{w}_{\text{gsc}}^H(\theta_k)\mathbf{w}_{\text{gsc}}(\theta_k)\sigma_n^2$. The GSC output SNR is $P_{\text{s}}/P_{\text{n}}$.

Taking into consideration a DOA estimation error ψ_k between the actual DOA θ_k and the estimated DOA $\hat{\theta}_k$ at time k (i.e., $\psi_k = \theta_k - \hat{\theta}_k$), each element in the steering vector becomes

$$a_p(\theta_k) = e^{-jp\kappa\sin(\hat{\theta}_k+\psi_k)}, \tag{10}$$

where we set $\kappa = \frac{2\pi}{\lambda}d$ for simplicity. If ψ_k is sufficiently small, then we have $\sin(\hat{\theta}_k + \psi_k) \approx \sin(\hat{\theta}_k) + \psi_k\cos(\hat{\theta}_k)$. Consequently, (10) can be rewritten as

$$a_p(\theta_k) = e^{-jp\kappa\sin(\hat{\theta}_k)} \cdot e^{-jp\kappa\psi_k\cos(\hat{\theta}_k)}. \tag{11}$$

As shown in (11), each element of the actual steering vector equals that of the estimated steering vector multiplied by the DOA error term $e^{-jp\kappa\psi_k\cos(\hat{\theta}_k)}$. To observe the influence of ψ_k in the GSC, we can expand the DOA error term with the following Taylor series as

$$\begin{aligned} e^{-jp\kappa\psi_k\cos(\hat{\theta}_k)} &= \sum_{n=0}^{\infty}(-1)^n\frac{\left[jp\kappa\psi_k\cos(\hat{\theta}_k)\right]^n}{n!} \\ &\approx 1 - jp\kappa\psi_k\cos(\hat{\theta}_k). \end{aligned} \tag{12}$$

Using (12), we can express (11) as

$$a_p(\theta_k) = a_p(\hat{\theta}_k) + e_{a,p}(\hat{\theta}_k), \tag{13}$$

where

$$e_{a,p}(\hat{\theta}_k) = -jp\kappa\psi_k\cos(\hat{\theta}_k)a_p(\hat{\theta}_k). \tag{14}$$

Let $\mathbf{e_a}(\hat{\theta}_k) = [e_{a,0}(\hat{\theta}_k), e_{a,1}(\hat{\theta}_k), \cdots, e_{a,P-1}(\hat{\theta}_k)]^T$. In light of (4) and (13), the estimated GSC beamforming vector $\mathbf{f}(\hat{\theta}_k)$ is

$$\begin{aligned} \mathbf{f}(\hat{\theta}_k) &= \frac{1}{P}\mathbf{a}(\hat{\theta}_k) \\ &= \frac{1}{P}\mathbf{a}(\theta_k) - \frac{1}{P}\mathbf{e_a}(\hat{\theta}_k) \\ &= \mathbf{f}(\theta_k) + \mathbf{e_f}(\hat{\theta}_k), \end{aligned} \tag{15}$$

where

$$\begin{aligned} \mathbf{e_f}(\hat{\theta}_k) &\triangleq [e_{f,0}(\hat{\theta}_k), e_{f,1}(\hat{\theta}_k), \cdots, e_{f,P-1}(\hat{\theta}_k)]^T \\ &= \frac{j\kappa\psi_k}{P}\cos(\hat{\theta}_k)[0, a_1(\hat{\theta}_k), \cdots, (P-1)a_{P-1}(\hat{\theta}_k)]^T. \end{aligned} \tag{16}$$

From (5) and (13), the estimated blocking matrix $\mathbf{B}(\hat{\theta}_k)$ becomes

$$\mathbf{B}(\hat{\theta}_k) = \mathbf{B}(\theta_k) + \mathbf{E_B}(\hat{\theta}_k), \tag{17}$$

where

$$\mathbf{E_B}(\hat{\theta}_k) = j\kappa\psi_k\cos(\hat{\theta}_k)\begin{bmatrix} \frac{a_1^*(\hat{\theta}_k)}{a_0^*(\hat{\theta}_k)} & \cdots & \frac{(P-1)a_{P-1}^*(\hat{\theta}_k)}{a_0^*(\hat{\theta}_k)} \\ 0 & \cdots & 0 \\ \vdots & \ddots & \vdots \\ 0 & \cdots & 0 \end{bmatrix}. \tag{18}$$

By substituting (15) and (17) into $\mathbf{w}_{\text{gsc}}(\theta_k)$ in (6), the GSC output error signal in terms of the estimated DOA becomes

$$\begin{aligned} e_k &= \mathbf{w}_{\text{gsc}}^H(\hat{\theta}_k)\mathbf{r}_k \\ &= \mathbf{w}_{\text{gsc}}^H(\theta_k)\mathbf{r}_k + \left[\mathbf{e_f}(\hat{\theta}_k) - \mathbf{E_B}(\hat{\theta}_k)\mathbf{w}_k\right]^H\mathbf{r}_k \\ &= s_k + \varepsilon_k \end{aligned} \tag{19}$$

where

$$\varepsilon_k = \mathbf{w}_{\text{gsc}}^H(\theta_k)\mathbf{n}_k + [\mathbf{e_f}(\hat{\theta}_k) - \mathbf{E_B}(\hat{\theta}_k)\mathbf{w}_k]^H\mathbf{r}_k. \tag{20}$$

From (19) and (20), we can see that the DOA mismatch ψ_k results in an extra term $[\mathbf{e_f}(\hat{\theta}_k) - \mathbf{E_B}(\hat{\theta}_k)\mathbf{w}_k]^H\mathbf{r}_k$, which increases the noise power. The overall output power then becomes $P_e = P_{\text{s}} + P_{\text{n}} + P_\psi$, where P_ψ denotes the power of the ψ_k-related term $[\mathbf{e_f}(\hat{\theta}_k) - \mathbf{E_B}(\hat{\theta}_k)\mathbf{w}_k]^H\mathbf{r}_k$. Hence, the GSC output SNR with DOA mismatch decreases to $P_{\text{s}}/(P_{\text{n}} + P_\psi)$.

B. DOA Estimation of a GSC

Suppose that the location of the target source is time varying. Our idea goes to that the effect of the DOA mismatch at the GSC output can be explored estimate the DOA. However, we also assume that a proper initial DOA is given before the following GSC tracking algorithm begins to operate.

Consider choosing an appropriate number of K samples over the interval $[k, k+K-1]$ such that the input signal s_k can be approximated as zero mean. From (19) and (20), we obtain the K samples of the average of e_n as follows:

$$\begin{aligned} \bar{e}_k &= \sum_{n=k}^{k+K-1} e_n \\ &= \sum_{n=k}^{k+K-1} s_n + \sum_{n=k}^{k+K-1}\mathbf{w}_{\text{gsc}}^H(\theta_k)\mathbf{n}_k \\ &\quad + \sum_{n=k}^{k+K-1}\left[\mathbf{e_f}(\hat{\theta}_n) - \mathbf{E_B}(\hat{\theta}_n)\mathbf{w}_n\right]^H\mathbf{r}_n \\ &\simeq \sum_{n=k}^{k+K-1}\left[\mathbf{e_f}(\hat{\theta}_n) - \mathbf{E_B}(\hat{\theta}_n)\mathbf{w}_n\right]^H\mathbf{r}_n. \end{aligned} \tag{21}$$

Using (14)−(18), $\left[\mathbf{e_f}(\hat{\theta}_n) - \mathbf{E_B}(\hat{\theta}_n)\mathbf{w}_n\right]^H\mathbf{r}_n$ in (21) can be rearranged as

$$\begin{aligned} &\left[\mathbf{e_f}(\hat{\theta}_n) - \mathbf{E_B}(\hat{\theta}_n)\mathbf{w}_n\right]^H\mathbf{r}_n \\ &= j\kappa\psi_n\cos(\hat{\theta}_n)\sum_{p=1}^{P-1}p\left[a_p(\hat{\theta}_n)w_{p-1,n}^*r_{0,n} - \frac{1}{P}a_p^*(\hat{\theta}_n)r_{p,n}\right] \\ &= \psi_n\epsilon_n, \end{aligned} \tag{22}$$

where

$$\epsilon_n = j\kappa\cos(\hat{\theta}_n)\sum_{p=1}^{P-1}p\left[a_p(\hat{\theta}_n)w_{p-1,n}^*r_{0,n} - \frac{1}{P}a_p^*(\hat{\theta}_n)r_{p,n}\right]. \tag{23}$$

The detailed derivations (22)−(23) can be found in the Appendix.

In practice, the DOA mismatch ψ_n can be modeled as $\psi_n = \bar{\psi}_k + \triangle\psi_n$ for typical source motion, where $\bar{\psi}_k$ is a constant value over $n = k, k+1, \cdots, k+K-1$ and $\triangle\psi_n$ represents a random noise. That is, $\bar{\psi}_k$ can be considered the average value of the DOA mismatch at index k over the K samples.[1] For simplicity, we assume $\triangle\psi_n \sim N(0, \sigma_\psi^2)$. Thus, (21) becomes

$$\bar{e}_k \simeq \bar{\psi}_k\sum_{n=k}^{k+K-1}\epsilon_n + \sum_{n=k}^{k+K-1}\triangle\psi_n\epsilon_n. \tag{24}$$

By neglecting the last term on the right side of (24), we have

$$\bar{\psi}_k \simeq \frac{\sum_{n=k}^{k+K-1}e_n}{\sum_{n=k}^{k+K-1}\epsilon_n}. \tag{25}$$

[1]This is a delay of approximately $K/2$ samples. However, this delay can be ignored if the sampling rate is sufficiently high.

Because ψ_k is a phase that is a real number, we simply choose

$$\hat{\psi}_k = \mathcal{R}e\{\bar{\psi}_k\}, \tag{26}$$

where $\mathcal{R}e\{\cdot\}$ denotes taking the real part and neglect the imaginary part of $\bar{\psi}_k$ as the noisy turbulence.

To prevent the numerical problem in computing (25) as a result of the measurement noise possibly generating a denominator value close to zero, we may improve the estimation robustness by replacing $\hat{\psi}_k$ with $\phi(\hat{\psi}_k)$, where $\phi(\cdot)$ is a limit function defined as $\phi(x) = x$ if $|x| \le \xi$ and $\phi(x) = 0$ if $|x| > \xi$, where ξ is a predetermined threshold. Next, we use the following recursion to estimate θ_k:

$$\hat{\theta}_{k+K} = \hat{\theta}_k + \mu_\theta \phi(\hat{\psi}_k), \tag{27}$$

where μ_θ is a step size that controls the estimate of the DOA. Although it seldom occurs that $\hat{\psi}_k$ abruptly becomes large in the recursion, we may treat the estimate as a numerical defect when $\hat{\psi}_k$ exceeds the threshold ξ. In this case, we simply omit the dubious estimate and maintain the estimate from the last result (i.e., $\hat{\theta}_{k+K} = \hat{\theta}_k$). Although the proposed algorithm calculates the DOA every K samples, it is satisfactory for our simulation cases because the sample frequency can be sufficiently high with a modern DSP specification. Additionally, the DOA estimates between $k+1$ and $k+K-1$ can be approximated by employing a simple extrapolation method with the results obtained from (27).

IV. AKF Beamforming Algorithm

A. Conventional Adaptive Beamforming Algorithms

Although the Wiener solution is optimal for the GSC problem given an accurate DOA, the matter of most critical interest is how to implement the theoretical autocovariance matrix $\mathbf{R_{rr}}$ in (8). For a fixed target source, the statistics of $\mathbf{R_{rr}}$ can be approximated by the ensemble average as follows:

$$\mathbf{R}_{rr,k} = (1-\beta)\mathbf{R}_{rr}, k-1 + \beta \mathbf{r}_k \mathbf{r}_k^H, \tag{28}$$

where $0 < \beta \le 1$ is a forgetting factor with a value that is usually almost zero and $\mathbf{R}_{rr,k}$ can converge to $\mathbf{R}_{rr}$ as k approaches infinity. However, if the target source is moving, then obtaining a satisfying result for approaching $\mathbf{R_{rr}}$ with this method is difficult.

Some adaptive filters such as the LMS filter, RLS filter, and KF are typical recursive filters that can be adopted to estimate $\mathbf{w}_k$. For example [14], the KF models $\mathbf{w}_k$ as the state vector and d_k^* as the observation; consequently, we obtain the following state and observation equations for the KF:

$$\mathbf{w}_{k+1} = \mathbf{w}_k + \boldsymbol{\omega}_k, \tag{29}$$

$$d_k^* = \mathbf{b}_k^H \mathbf{w}_k + \delta_k, \tag{30}$$

where $\boldsymbol{\omega}_k$ and δ_k are modeled as the zero-mean white Gaussian processes. However, the conventional KF used in the GSC can be applied satisfactorily only under the condition that e_k contains a small amount of white noise. In the case where e_k contains the desired signal s_k in addition to white noise, a large estimation error variance of δ_k degrades the convergence performance. In this section, we develop a state-augmented method for the KF to avoid GSC performance degradation.

B. AKF Algorithm

Suppose that the complex signal s_k in (3) is represented as $s_k = \tilde{s}_k e^{j\phi_k}$, where ϕ_k is the phase of s_k and the envelope $\tilde{s}_k$ is usually characterized by a low pass signal. For simplicity, $\tilde{s}_k$ is modeled as an L-order autoregressive (AR) process

$$\tilde{s}_k = \sum_{l=1}^{L} \alpha_l \tilde{s}_{k-l} + \xi_k, \tag{31}$$

where α_l is the AR coefficient and ξ_k is a zero-mean white noise with variance σ_ξ^2 and ϕ_k can be modeled as a Wiener process.

$$\phi_{k+1} = \phi_k + \eta_k, \tag{32}$$

where η_k is a zero-mean white Gaussian noise with variance σ_η^2. Using the mentioned signal model, we develop the AKF to improve the beamfoming performance, where the desired signal s_k can be estimated and canceled from the observation equation to reduce the estimation error variance.

To simplify the problem, we consider $L = 2$ for the AR signal given the coefficients α_1 and α_2. Next, define the $(P+2)\times 1$ state vector $\mathbf{x}_k = [\tilde{s}_k \ \tilde{s}_{k-1} \ \phi_k \ \mathbf{w}_k^T]^T$ and the observation vector $[d_k^* \ e_k]^T$. Here, the state vector is augmented by introducing $\tilde{s}_k$, $\tilde{s}_{k-1}$, and ϕ_k in addition to $\mathbf{w}_k^T$. Subsequently, we construct the state and measurement equations for the AKF as

$$\mathbf{x}_{k+1} = \Phi \mathbf{x}_k + \mathbf{u}_k \tag{33}$$

and

$$\begin{bmatrix} d_k^* \\ e_k \end{bmatrix} = \begin{bmatrix} h(\mathbf{x}_k) \\ g(\mathbf{x}_k) \end{bmatrix} + \begin{bmatrix} v_{1k} \\ v_{2k} \end{bmatrix}, \tag{34}$$

respectively, where

$$\Phi = \begin{bmatrix} \alpha_1 & \alpha_2 & 0 & \mathbf{0} \\ 1 & 0 & 0 & \mathbf{0} \\ 0 & 0 & 1 & \mathbf{0} \\ 0 & 0 & 0 & \mathbf{I} \end{bmatrix}, \tag{35}$$

$$h(\mathbf{x}_k) = \mathbf{b}_k^H \mathbf{w}_k + \tilde{s}_k e^{j\phi_k}, \tag{36}$$

$$g(\mathbf{x}_k) = \tilde{s}_k e^{j\phi_k}, \tag{37}$$

and $\mathbf{u}_k$ is the white zero-mean Gaussian process noise vector with covariance matrix $Q_k = \mathrm{diag}[\sigma_\xi^2 \ 0 \ \sigma_\eta^2 \ \sigma_w^2 \mathbf{I}]$, $[v_{1k} \ v_{2k}]^T$ is the zero-mean white Gaussian observation noise vector with covariance matrix $R_k = \mathrm{diag}[\sigma_v^2 \ \sigma_v^2]$, $\mathbf{0}$ is the $1 \times (P-1)$ zero column vector, and $\mathbf{I}$ is the $(P-1)\times(P-1)$ identity matrix. Because $h(\mathbf{x}_k)$ and $\tilde{s}_k e^{j\phi_k}$ are nonlinear functions of $\mathbf{x}_k$, the extended KF is employed to estimate $\mathbf{x}_k$ with the following recursions:

$$i\hat{\mathbf{x}}_{k+1|k} = \Phi \hat{\mathbf{x}}_{k|k}, \tag{38}$$

$$\hat{P}_{k+1|k} = \Phi \hat{P}_{k|k} \Phi^H + Q_k, \tag{39}$$

$$G_{k+1} = \frac{\hat{P}_{k+1|k} H_{k+1}^H}{H_{k+1} \hat{P}_{k+1|k} H_{k+1}^H + R_{k+1}}, \tag{40}$$

$$\hat{\mathbf{x}}_{k+1|k+1} = \hat{\mathbf{x}}_{k+1|k} + G_{k+1} \left(\begin{bmatrix} d_{k+1}^* \\ e_{k+1} \end{bmatrix} - \begin{bmatrix} h(\hat{\mathbf{x}}_{k+1|k}) \\ g(\hat{\mathbf{x}}_{k+1|k}) \end{bmatrix} \right), \tag{41}$$

$$\hat{P}_{k+1|k+1} = (\mathbf{I} - G_{k+1} H_{k+1}) \hat{P}_{k+1|k}, \tag{42}$$

TABLE I
SIMULATION SETUP

Parameters	Values
Number of arrays (P)	16
Sensor spacing (d)	$\frac{\lambda}{2}$
Sampling rate (S), in KHz	20
Number of average samples (K)	10
Threshold of limit function (ξ)	0.35°
Simulation time (in seconds)	10
DOA of the desired signal	case 1: 0° case 2: 0° to 70° case 3: $-14^\circ \sim 14^\circ$
DOA of interfering signals	case 1: $-10^\circ, 15^\circ, 50^\circ$ case 2: $-10^\circ, 15^\circ, 50^\circ$ case 3: $-7^\circ, 30^\circ, -50^\circ$
SNR	30 dB
SIR	20 dB, 20 dB, 20 dB
Background noise	AWGN

where $\mathbf{I}$ is the $(P+2)\times(P+2)$ identity matrix and H_{k+1} is the Jacobian matrix of $[h(\hat{\mathbf{x}}_{k+1|k})\ g(\hat{\mathbf{x}}_{k+1|k})]^T$; in other words,

$$H_{k+1} = \left.\frac{\partial[h(\mathbf{x}_{k+1})\ g(\mathbf{x}_{k+1})]^T}{\partial\ \mathbf{x}_{k+1}}\right|_{\mathbf{x}_{k+1}=\hat{\mathbf{x}}_{k+1|k}} = \begin{bmatrix} e^{j\phi_{k+1|k}} & 0 & j\tilde{s}_{k+1|k}e^{j\phi_{k+1|k}} & \mathbf{b}_{k+1}^H \\ e^{j\phi_{k+1|k}} & 0 & j\tilde{s}_{k+1|k}e^{j\phi_{k+1|k}} & \mathbf{0} \end{bmatrix}, \quad (43)$$

where $\hat{\theta}_{k+1}$ in $\mathbf{b}_{k+1}$ is obtained from (27).

V. SIMULATION RESULTS

To study the effectiveness of the proposed DOA tracking method, we evaluated the SINR performance for different adaptive GSC algorithms along with the proposed DOA estimation method. From (19), the theoretical SINR is defined as

$$\text{SINR} = \frac{\mathbb{E}[|s_k|^2]}{\mathbb{E}[|\varepsilon_k|^2]}. \quad (44)$$

To calculate the SINR through simulations, we first considered the instantaneous SINR at the kth snapshot, which can be written as

$$\text{SINR}_k(i) = \frac{|s_k(i)|^2}{|e_k(i) - s_k(i)|^2}, \quad i = 1, 2, \cdots, M \quad (45)$$

where the index i represents the ith Monte Carlo simulation and M is the total number of Monte Carlo simulations. Subsequently, the ensemble average SINR is calculated from the results of the M Monte Carlo simulations,

$$\text{SINR}_k = \frac{1}{M}\sum_{i=1}^{M}\text{SINR}_k(i). \quad (46)$$

For SINR performance evaluation, the proposed AKF algorithm is compared with two typical adaptive beamforming algorithms that have similar computational complexity, the RLS [13] and KF [15] algorithms, when combined with the proposed DOA tracking method for a moving target signal source. Table I details the parameter setup for our simulations.

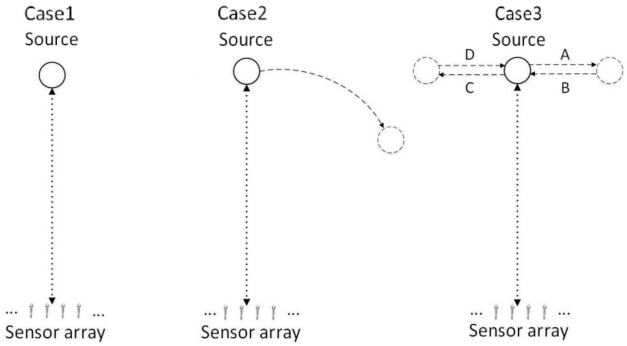

Fig. 3. Motion scenarios of the target signal source.

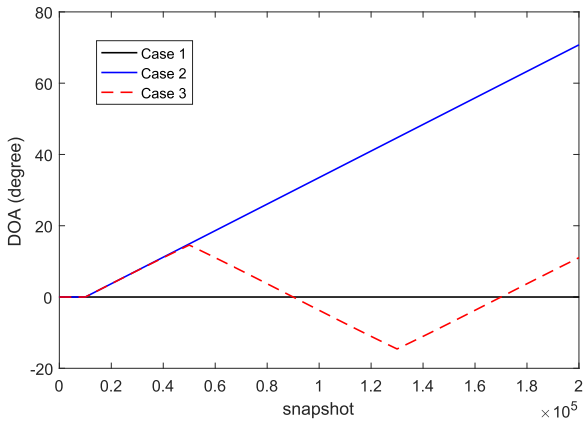

Fig. 4. DOA of the target signal source for the three simulation cases.

We consider three motion scenarios of the target signal source as the moving paths depicted in Fig. 3: staying fixed (Case 1), going forward (Case 2), and going back and forth (Case 3). We assume there to be three random stationary interfering signals moving in different directions. In Cases 2 and 3, the target source assumes a constant velocity motion. Fig. 4 shows the variation of the angles to be tracked in the three simulation cases. For example, in Case 2, we assume that the sound source makes a circular motion within 9.5 s (the initial 0.5 s is stable) to achieve a 10-s movement record. Thus, we have a total of 200 K samples with a sample rate of 20 KHz.

We set an initial θ_0 value for (27), and the target source starts moving after 0.5 s. A small bias of the initial θ_0 within a few degrees does not cause a severe convergence problem in the GSC algorithms. During this initial phase, the adaptive GSC algorithms boost the estimation of their beamforming weighting coefficients. As the target source moves, the output signal e_k of the GSC increases such that (25) can lead to updating θ_k from (27). Case 2 in Fig. 4 demonstrates that the motion results in an angle change of approximately 0.0035° for every $K = 10$ samples. Next, setting the threshold $\xi = 0.35^\circ$ for the limit function in (27) means that if the estimate $\hat{\psi}_k$ has a tolerance that is more than 100 times greater than the typical angle change, then we ignore the estimate because the error is considered to be too large. Here, the desired signal modeled in (31) assumes that $\tilde{s}_k$ is an AR(2) process with coefficients $\alpha_1 = 1.2728$, $\alpha_2 = -0.81$, and $\sigma_\xi^2 = 1$. The received signal for each sensor is simulated with three interfering signals that have a signal-to-interference power

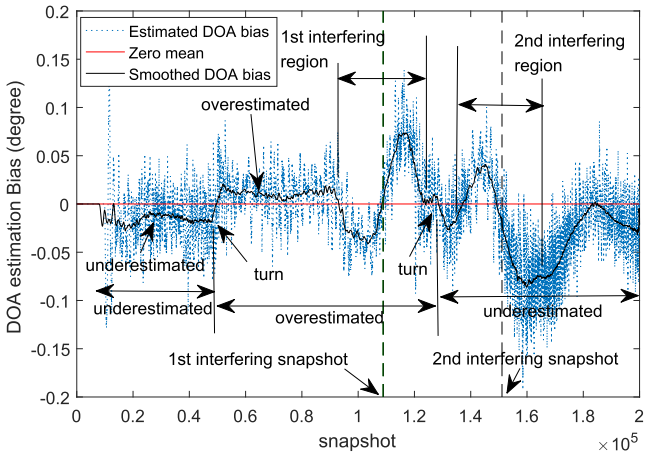

Fig. 5. DOA estimation bias due to estimation lag caused by the average operation over K samples in Case 3.

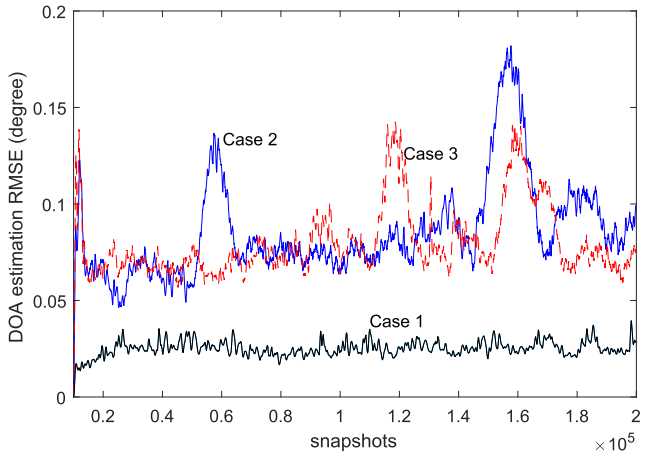

Fig. 6. DOA estimation RMSE of the target source for the three simulation cases.

ratio (SIR) of 20 dB and background AWGN with an SNR of 30 dB.

A. DOA Estimation

Although the proposed DOA tracking algorithm can produce an unbiased estimate for a fixed target source, a small amount of estimation bias cannot be avoided for a time-varying DOA because of the average operation (low pass filtering) over K samples. However, almost no SINR degradation observed from our simulation results because of the remarkably little DOA estimation bias. Fig. 5 shows, as an example, the DOA estimation bias for the AKF algorithm in Case 3. In Case 3, the target source makes two turns, specifically at snapshots 0.5×10^5 and 1.3×10^5. Because the average operation can lead to an estimation lag with respect to the actual DOA with a DOA change rate of approximately 7°/s, a small underestimation bias of less than 0.025° can be observed before snapshot 0.5×10^5 and after snapshot 1.3×10^5. Between snapshots 0.5×10^5 and 1.3×10^5, an overestimation bias is observed. In addition, two regions of larger estimation bias appear when the target source moves in the directions of the interfering signals because the desired signal is destroyed by the interfering signals.

Figure 6 plots the root mean square error (RMSE) of DOA estimation of the three cases with the proposed DOA tracking method for the AKF algorithm. As illustrated in Fig. 6, the target source in Case 1 remains fixed such that the RMSE is approximately 0.025°. For Cases 2 and 3, the moving source leads to a worse RMSE than that for Case 1 because the GSC output error signal has a larger variance when the target source moves. Larger estimation RMSE is caused by larger DOA estimation bias due to interfering signals; for example, in Case 3, two RMSE peaks occur near snapshots 1.2×10^5 and 1.6×10^5. Although the DOA tracking performance is degraded as the target source moves in the directions of interfering signals, the estimation accuracy remains within a 0.2° RMSE and does not result in tracking failure, even though a performance loss of SIR 15 dB is caused by the interfering signals. According to the results of the simulation analysis of SIR performance, the estimation accuracy of the proposed DOA tracking method is satsfactory for the GSC with a direction change rate of 7°/s.

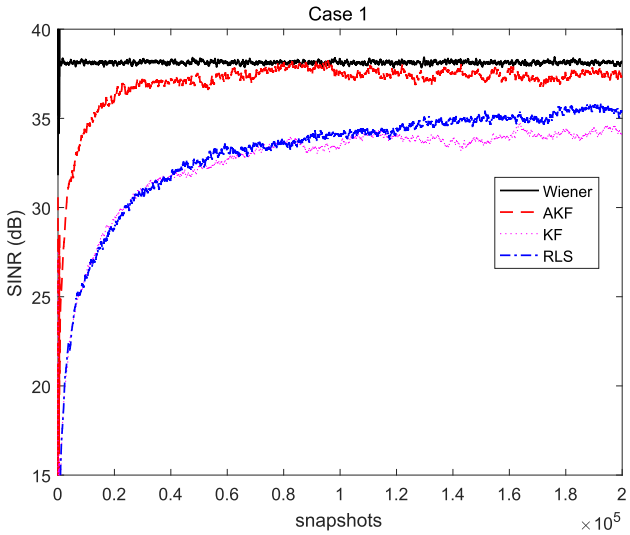

Fig. 7. SINR performance of the adaptive beamforming algorithms employed with the proposed DOA tracking method for Case 1.

B. SINR Performance

Case 1: In Case 1, we consider the location of the target source to be fixed in the direction of 0°. Assume that three interfering signals are located at the directions of −10°, 15°, and 50°. We then compare the SINR performance of AKF, KF, and RLS algorithms when combined with the proposed DOA estimation method. The results are shown in Fig. 7, where the performance of the Wiener solution with a known DOA is also plotted as the performance bound. Apparently, the AKF algorithm reasonably demonstrates better SINR performance than the RLS and KF algorithms because the source signal s_k is removed from the GSC output error signal. When combined with the proposed DOA tracking method, the steady-state SINR performance of the AKF shows almost no degradation. However, the RLS and KF algorithms have a small SINR performance degradation. The main reason for this performance degradation is that the AKF algorithm removes the desired

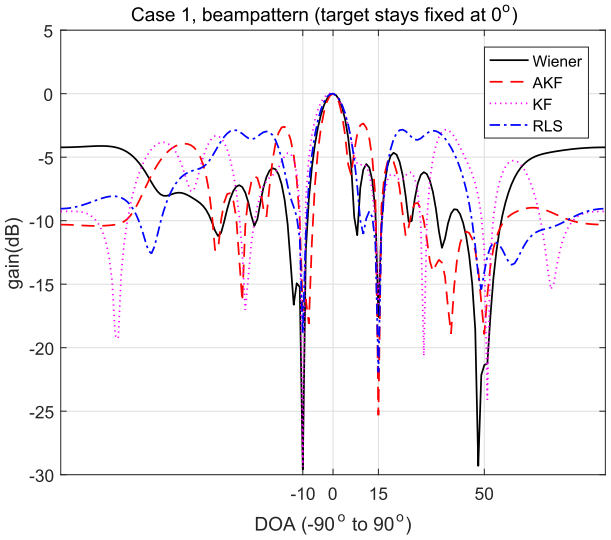

Fig. 8. Beam pattern of the adaptive beamforming algorithms for Case1. Three interfering signals are located in the directions of −10°, 15°, and 50°.

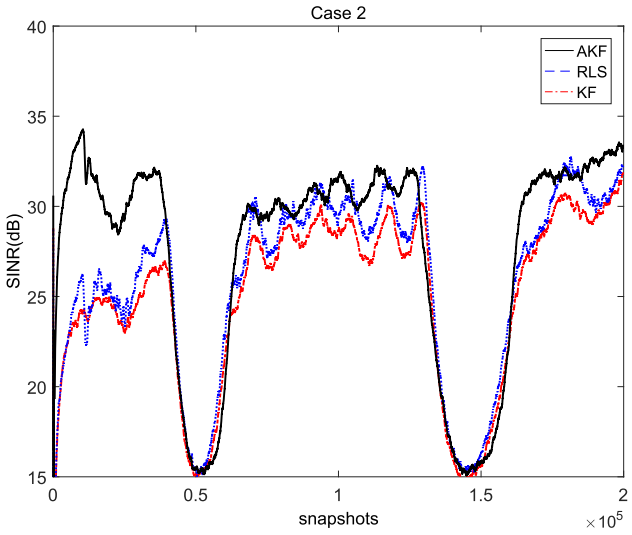

Fig. 9. SINR performance of the three adaptive beamforming algorithms with the proposed DOA tracking method for Case 2.

signal from the GSC output such that a smaller GSC output error signal improves the convergence performance.

Fig. 8 displays the beam patterns of the Wiener solution, AKF, RLS, and KF beamforming algorithms. Notably, the target source remains fixed in the direction of 0°, and three interfering signals are moving in the directions of −10°, 15°, and 50°. All of the beam patterns exhibit three common nulls in the directions of interfering signals and maintain the unity gain at 0°, indicating that the three algorithms can emphasize the received signal in the direction of the target source and properly eliminate the interference in the directions of the interfering signals.

Case 2: Fig. 9 presents the SINR performance of the AKF, KF, and RLS algorithms in Case 2, all combined with the proposed DOA tracking method. Because the Wiener solution requires the stationary value $\mathbf{R_{rr}}$ of the input signal $\mathbf{r}_k$, which varies with the DOA, the SINR becomes poor when the target DOA is time-varying; consequently, its performance is

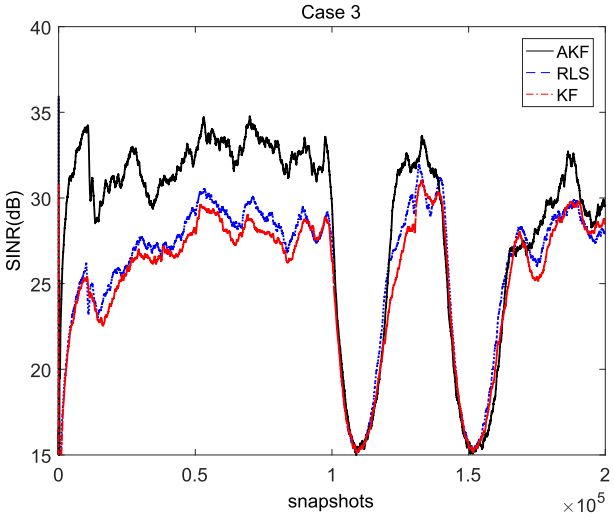

Fig. 10. SINR performance of the three adaptive beamforming algorithms with the proposed DOA tracking method for Case 3.

not plotted for comparison. If DOA tracking is not implemented for the adaptive GSC algorithms, then all of the adaptive algorithms demonstrate severe performance degradation because the DOA has a mismatch of 7°/s in this case. The AKF algorithm exhibits noticeably better performance, namely because the error signal for the adaptation does not contain the desired signal such that the weighting vector $\mathbf{w}_k$ can be better estimated to cancel out interfering signals. Because two interfering signals are present on the trajectory of the moving target source, an SINR performance degradation of approximately 15 dB can be observed at two points. The first degradation point has a duration of approximately 1.31 s, and the second one has a duration of approximately 1.77 s. The second null takes longer than the first because the angular resolution (3-dB gain) of the ULA beamformer has a greater negative effect at 50° than at 15°, leading the 50° interfering signal to demonstrate a longer interference duration than the 15° interfering signal for circular motion at a constant speed.

Case 3: Fig. 10 compares the SINR performance of all algorithms used in combination with the proposed DOA tracking method for Case 3. In this case, the target source moves twice through the interfering signal in the direction of −7°. Each of the two nulls takes approximately 1.23 s of the 10-s trajectory. The AKF still achieves better SINR performance than do the RLS and KF algorithms.

C. Influence of the Main System Parameters

We next explore the influence of the system parameters, namely sampling rate S and number of arrays P, by using the AKF algorithm with the proposed DOA tracking method with the simulation setup of Case 2.

Because the adaptive beamforming algorithms require a sufficient number of samples to calculate the beamforming coefficients for a time-varying DOA to achieve satisfactory SINR performance, the sampling rate depends on the movement speed of the target source. In our simulation, the source has a speed of approximately 7°/s. Figure 11 shows that an SINR greater than 30 dB can be reached for the entire

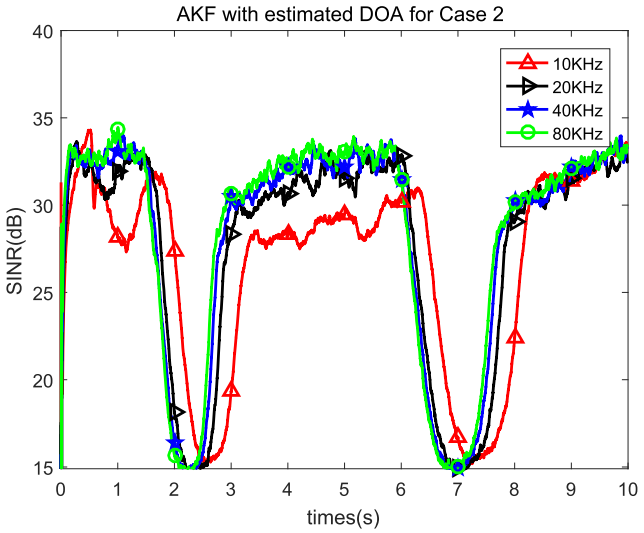

Fig. 11. SINR of the AKF algorithm for different sampling rates.

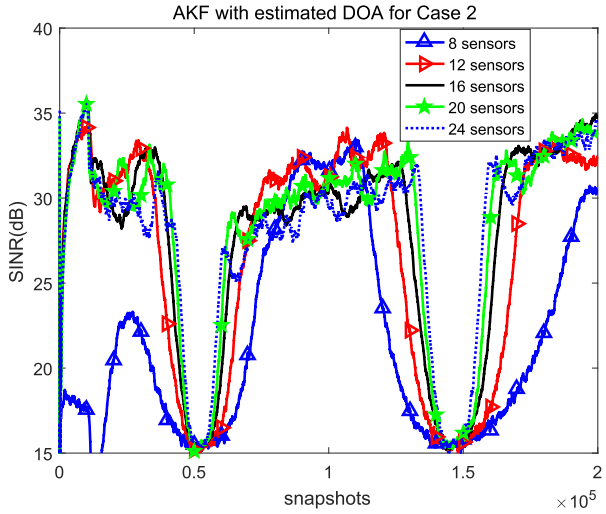

Fig. 12. SINR of the AKF algorithm for different numbers of sensors.

simulation duration with a sampling rate exceeding 20 KHz. If $S = 10$KHz, then slow response and performance degradation can be observed from the SINR evaluation. If S is larger than 20 KHz, then the SINR performance does not improve significantly.

The vector size of the beamforming coefficient $\mathbf{w}_k$ is related to the number of sensors P; that is, the resolution of the beamformer is determined by P. Figure 12 shows the SINR performance of the AKF algorithm for different P values. In our simulation setup, $P = 8$ results in insufficient resolution, thus causing considerable performance degradation in the directions of interfering signals. As the number of sensors increases, the duration of performance degradation decreases. Although increasing P can improve the SINR performance, the cost is also increased. In our simulation cases, because P is larger than 16, no significant difference in performance is observed.

VI. Conclusion

This study proposes a new DOA tracking method and AKF algorithm for GSC beamforming that can be applied to sensor arrays for enhancing the signal of a moving target source when received along with interfering signals. The SNR analysis of the GSC in the presence of a DOA mismatch demonstrates that a DOA mismatch reduces the SNR of the GSC. The proposed DOA tracking method does not involve the large amount of computation required by conventional offline DOA estimation algorithms such as the MUSIC algorithm or ESPRIT; hence, the computational load of DSP for DOA estimation can be reduced. The new AKF algorithm improves GSC convergence performance by eliminating the influence of the desired signal from the GSC output error signal. The simulation results indicate that the AKF algorithm combined with the proposed DOA method achieves better SINR performance than the KF and RLS algorithms.

Appendix
Derivations of (22)–(23)

First consider the term $\mathbf{E_B}(\hat{\theta}_n)\mathbf{w}_n$ in (21). By using (18) and $a_0^*(\hat{\theta}_k) = 1$, we obtain

$$\begin{aligned}\mathbf{E_B}(\hat{\theta}_n)\mathbf{w}_n &= j\kappa\psi_n\cos(\hat{\theta}_n)\\ &\quad\times\begin{bmatrix} a_1^*(\hat{\theta}_n) & \cdots & (P-1)a_{P-1}^*(\hat{\theta}_n)\\ 0 & \cdots & 0\\ 0 & \cdots & 0\\ \vdots & \ddots & \vdots\\ 0 & \cdots & 0\end{bmatrix}\times\begin{bmatrix} w_{0,n}\\ w_{1,n}\\ \vdots\\ w_{P-2,n}\end{bmatrix}\\ &= j\kappa\psi_n\cos(\hat{\theta}_n)\begin{bmatrix}\sum_{p=1}^{P-1} pa_p^*(\hat{\theta}_n)w_{p-1,n}\\ 0\\ \vdots\\ 0\end{bmatrix}. \end{aligned}\quad (47)$$

Hence,

$$\begin{aligned}&\mathbf{e_f}(\hat{\theta}_n) - \mathbf{E_B}(\hat{\theta}_n)\mathbf{w}_n\\ &= \begin{bmatrix} e_{f,0}(\hat{\theta}_n) - j\kappa\psi_n\cos(\hat{\theta}_n)\sum_{p=1}^{P-1} pa_p^*(\hat{\theta}_n)w_{p-1,n}\\ e_{f,1}(\hat{\theta}_n)\\ \vdots\\ e_{f,P-1}(\hat{\theta}_n).\end{bmatrix},\end{aligned}\quad (48)$$

which can be rewritten as follows by using (14) and (15):

$$\begin{aligned}&\left[\mathbf{e_f}(\hat{\theta}_n) - \mathbf{E_B}(\hat{\theta}_n)\mathbf{w}_n\right]^H\mathbf{r}_n\\ &= \begin{bmatrix} e_{f,0}(\hat{\theta}_n) - j\kappa\psi_n\cos(\hat{\theta}_n)\sum_{p=1}^{P-1} pa_p^*(\hat{\theta}_n)w_{p-1,n}\\ e_{f,1}(\hat{\theta}_n)\\ \vdots\\ e_{f,P-1}(\hat{\theta}_n)\end{bmatrix}^H\\ &\quad\times\begin{bmatrix} r_{0,n}\\ r_{1,n}\\ \vdots\\ r_{P-1,n}\end{bmatrix}\\ &= \left[e_{f,0}^*(\hat{\theta}_n)r_{0,n} + \cdots + e_{f,P-1}^*(\hat{\theta}_n)r_{P-1,n}\right]\\ &\quad + j\kappa\psi_n\cos(\hat{\theta}_n)\sum_{p=1}^{P-1} pa_p(\hat{\theta}_n)w_{p-1,n}^*r_{0,n}\end{aligned}$$

$$
\begin{aligned}
&= \frac{1}{P}\big[0 - j\kappa\psi_n \cos(\hat{\theta}_n) a_1^*(\hat{\theta}_k) r_{1,n} - \cdots \\
&\quad - j(P-1)\kappa\psi_n \cos(\hat{\theta}_n) a_{P-1}^*(\hat{\theta}_k) r_{P-1,n}\big] \\
&\quad + j\kappa\psi_n \cos(\hat{\theta}_n) \sum_{p=1}^{P-1} p a_p(\hat{\theta}_n) w_{p-1,n}^* r_{0,n} \\
&= -\frac{1}{P} \times j\kappa\psi_n \cos(\hat{\theta}_n) \sum_{p=1}^{P-1} p a_p^*(\hat{\theta}_n) r_{p,n} \\
&\quad + j\kappa\psi_n \cos(\hat{\theta}_n) \sum_{p=1}^{P-1} p a_p(\hat{\theta}_n) w_{p-1,n}^* r_{0,n} \\
&= j\kappa\psi_n \cos(\hat{\theta}_n) \sum_{p=1}^{P-1} p\big[a_p(\hat{\theta}_n) w_{p-1,n}^* r_{0,n} - \frac{1}{P} a_p^*(\hat{\theta}_n) r_{p,n}\big].
\end{aligned}
$$

REFERENCES

[1] B. Allen and M. Ghavami, *Adaptive Array Systems: Fundamentals and Applications*. Hoboken, NJ, USA: Wiley, 2005.

[2] L. Zhao, J. Benesty, and J. Chen, "Design of robust differential microphone arrays," *IEEE/ACM Trans. Audio, Speech, Language Process.*, vol. 22, no. 10, pp. 1455–1466, Oct. 2014.

[3] S. M. Kim and H. K. Kim, "Multi-microphone target signal enhancement using generalized sidelobe canceller controlled by phase error filter," *IEEE Sensors J.*, vol. 16, no. 21, pp. 7566–7567, Nov. 2016.

[4] L. Liu, Y. Li, and S. M. Kuo, "Feed-forward active noise control system using microphone array," *IEEE/CAA J. Automat. Sinica*, vol. 5, no. 5, pp. 946–952, Sep. 2018.

[5] M. F. A. Ahmed and S. A. Vorobyov, "Collaborative beamforming for wireless sensor networks with Gaussian distributed sensor nodes," *IEEE Trans. Wireless Commun.*, vol. 8, no. 2, pp. 638–643, Feb. 2009.

[6] M. Zohourian, G. Enzner, and R. Martin, "Binaural speaker localization integrated into an adaptive beamformer for hearing aids," *IEEE/ACM Trans. Audio, Speech, Language Process.*, vol. 26, no. 3, pp. 515–528, Mar. 2018.

[7] V. C. Gogineni and S. Mula, "Logarithmic cost based constrained adaptive filtering algorithms for sensor array beamforming," *IEEE Sensors J.*, vol. 18, no. 24, pp. 5897–5905, Jul. 2018.

[8] K. Buckley, "Broad-band beamforming and the generalized sidelobe canceller," *IEEE Trans. Acoust., Speech, Signal Process.*, vol. ASSP-34, no. 5, pp. 1322–1323, Oct. 1986.

[9] Z. Liu, S. Zhao, G. Zhang, and B. Jiao, "Robust adaptive beamforming for sidelobe canceller with null widening," *IEEE Sensors J.*, vol. 19, no. 23, pp. 11213–11220, Dec. 2019.

[10] O. L. Frost, III, "An algorithm for linearly constrained adaptive array processing," *Proc. IEEE*, vol. 60, no. 8, pp. 926–935, Aug. 1972.

[11] C. Yu and L. Su, "Speech enhancement based on the generalized sidelobe cancellation and spectral subtraction for a microphone array," in *Proc. 8th Int. Congr. Image Signal Process. (CISP)*, Oct. 2015, pp. 1318–1322.

[12] M. Triki, "Performance issues in recursive least-squares adaptive GSC for speech enhancement," in *Proc. IEEE Int. Conf. Acoust., Speech Signal Process.*, Apr. 2009, pp. 225–228.

[13] D. Comminiello, M. Scarpiniti, R. Parisi, and A. Uncini, "Combined adaptive beamforming techniques for noise reduction in changing environments," in *Proc. 36th Int. Conf. Telecommun. Signal Process. (TSP)*, Jul. 2013, pp. 690–694.

[14] F. Gomes, A. Neto, and A. De Araujo, "Kalman filter applied to GSC in adaptive antennas array," in *Proc. IEEE Radio Wireless Conf. (RAWCON)*, Sep. 2000, pp. 125–130.

[15] S. C. Tanan, K. Nathwani, A. Jain, R. M. Hegde, R. Rani, and A. Tripathy, "Acoustic echo and noise cancellation using Kalman filter in a modified GSC framework," in *Proc. 48th Asilomar Conf. Signals, Syst. Comput.*, Nov. 2014, pp. 477–481.

[16] C. Cui, W. Wu, and W.-Q. Wang, "Carrier frequency and DOA estimation of sub-Nyquist sampling multi-band sensor signals," *IEEE Sensors J.*, vol. 17, no. 22, pp. 7470–7478, Nov. 2017.

[17] X. Ma, X. Dong, and Y. Xie, "An improved spatial differencing method for DOA estimation with the coexistence of uncorrelated and coherent signals," *IEEE Sensors J.*, vol. 16, no. 20, pp. 3719–3723, May 2016.

[18] X. Zhong, A. B. Premkumar, and A. S. Madhukumar, "Particle filtering for acoustic source tracking in impulsive noise with alpha-stable process," *IEEE Sensors J.*, vol. 13, no. 2, pp. 589–600, Feb. 2013.

[19] F. Yan, M. Jin, and X. Qiao, "Low-complexity DOA estimation based on compressed MUSIC and its performance analysis," *IEEE Trans. Signal Process.*, vol. 61, no. 8, pp. 1915–1930, Apr. 2013.

[20] Z. Khan, M. M. D. Kamal, N. Hamzah, K. Othman, and N. I. Khan, "Analysis of performance for multiple signal classification (MUSIC) in estimating direction of arrival," in *Proc. IEEE Int. RF Microw. Conf.*, Dec. 2008, pp. 524–529.

[21] N. Yuen and B. Friedlander, "Asymptotic performance analysis of ESPRIT, higher order ESPRIT, and virtual ESPRIT algorithms," *IEEE Trans. Signal Process.*, vol. 44, no. 10, pp. 2537–2550, Oct. 1996.

[22] J. Steinwandt, F. Roemer, and M. Haardt, "Performance analysis of ESPRIT-type algorithms for non-circular sources," in *Proc. IEEE Int. Conf. Acoust., Speech Signal Process. (ICASSP)*, May 2013, pp. 3986–3990.

[23] J.-Y. Lee, R. E. Hudson, and K. Yao, "Acoustic DOA estimation: An approximate maximum likelihood approach," *IEEE Syst. J.*, vol. 8, no. 1, pp. 131–141, Mar. 2014.

[24] Y. Kong, C. Zeng, G. Liao, and H. Tao, "A new reduced-dimension GSC for target tracking and interference suppression," in *Proc. IEEE CIE Int. Conf. Radar*, Oct. 2011, pp. 785–788.

[25] J. Wen, X. Zhou, W. Zhang, and B. Liao, "Robust adaptive beamforming against significant angle mismatch," in *Proc. IEEE Radar Conf. (RadarConf)*, May 2017, pp. 713–716.

[26] H. Wan, H. Huang, B. Liao, and Z. Quan, "Robust beamforming against direction-of-arrival mismatch via signal-to-interference-plus-noise ratio maximization," in *Proc. 9th Int. Conf. Wireless Commun. Signal Process. (WCSP)*, Oct. 2017, pp. 1–5.

[27] M. Rahmani, M. H. Bastani, and S. Shahraini, "Two layers beamforming robust against direction-of-arrival mismatch," *IET Signal Process.*, vol. 8, no. 1, pp. 49–58, Jan. 2014.

[28] W. Zhang, S. Wu, and J. Wang, "Robust Capon beamforming in presence of large DOA mismatch," *Electron. Lett.*, vol. 49, no. 1, pp. 75–76, Jan. 2013.

[29] Y. Bar-Shalom, R. Li, and T. Kirubarajan, *Estimation With Applications to Tracking and Navigation*. Hoboken, NJ, USA: Wiley, 2001.

[30] A. Massoud and A. Noureldin, "Angle of arrival estimation based on warped delay-and-sum (WDAS) beamforming technique," in *Proc. OCEANS*, Sep. 2011.

[31] S. Gannot, D. Burshtein, and E. Weinstein, "Signal enhancement using beamforming and nonstationarity with applications to speech," *IEEE Trans. Signal Process.*, vol. 49, no. 8, pp. 1614–1626, Aug. 2001.

Dah-Chung Chang (Senior Member, IEEE) received the B.S. degree in electronic engineering from Fu Jen Catholic University, Taipei, in 1991, and the M.S. and Ph.D. degrees in electrical engineering from National Chiao Tung University, Hsinchu, Taiwan, in 1993 and 1998, respectively. In 1998, he joined Computer and Communications Research Laboratories, Industrial Technology Research Institute, Hsinchu. Since 2003, he has been a Faculty Member with the Department of Communication Engineering, National Central University (NCU), where he is currently a Professor. His recent research interests include multi-antenna and MIMO communications, transceiver design, and broad applications of adaptive signal processing and deep learning.

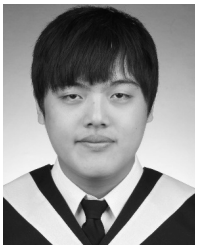

Bo-Wei Zheng received the M.S. degree in communication engineering from National Central University, Taoyuan, Taiwan, in 2016. Since graduation, he has been working with industries in signal processing and communications related fields. His research interests lie in the areas of signal processing and communication systems.